Simple and accurate analytical expressions for evaluating related transmission line integrals

2001 J. Phys. A: Math. Gen. 34 9027

(http://iopscience.iop.org/0305-4470/34/42/319)

INSTITUTE OF PHYSICS PUBLISHING JOURNAL OF PHYSICS A: MATHEMATICAL AND GENERAL

J. Phys. A: Math. Gen. **34** (2001) 9027–9035 PII: S0305-4470(01)18112-6

Simple and accurate analytical expressions for evaluating related transmission line integrals

A Maaouni[1]**, A Amri and A Zouhir**

Laboratoire D'Electronique, D'Electromagnétisme et d'Hyperfréquences. Université Hassan II, Faculté des Sciences Ain-Chock, Casablanca, BP 5336 Maârif, Morocco

Received 13 November 2000, in final form 8 August 2001
Published 12 October 2001
Online at stacks.iop.org/JPhysA/34/9027

Abstract

Simple and accurate analytical approximations of integrals relating to overhead transmission lines are presented in this paper. These approximations are valid for all arguments of the integrals and are faster in comparison with numerical integration.

PACS numbers: 02.30.-f, 02.60.-x, 84.40.Az

1. Introduction

In electromagnetic compatibility, transmission lines and cables are very important in assessing the interaction of an external stimulus (lightning, EMP, etc) to electrical systems. Transient electromagnetic energy is conducted through cables and may damage components in small-signal circuits. In determining how this energy distributes itself within systems, it is usually necessary to utilize the transmission line model. The basic assumptions in this model are that the response of the line is quasi-TEM and that the transverse dimensions of the line are small compared to the free space wavelength (thin wires). Under these assumptions, a system of horizontal wires parallel to the Earth's surface may be treated as a transmission line [1]. To allow for the possibility of determining the behaviour of complicated similar systems to external excitations, the transmission line characteristics have to be determined with less computational cost.

Using the quasi-TEM approach, it has been shown [2, 3] that the transmission line parameters, the series impedance and the shunt admittance per unit length, are expressible as a function of two integrals representing the conduction and the displacement current losses in the Earth. These integrals are approximations of the Sommerfeld integrals [4] under the quasi-TEM hypothesis. This paper gives a simple and precise analytic approximation of the two integrals in terms of logarithms and exponential integral functions. The comparison with the numerical integration shows that the analytical approximations are accurate for all typical arguments and are more rapid to evaluate.

[1] Present address: Hay Sadri, Rue 10, no 135, Groupe 3, 14001, Casablanca, Morocco.

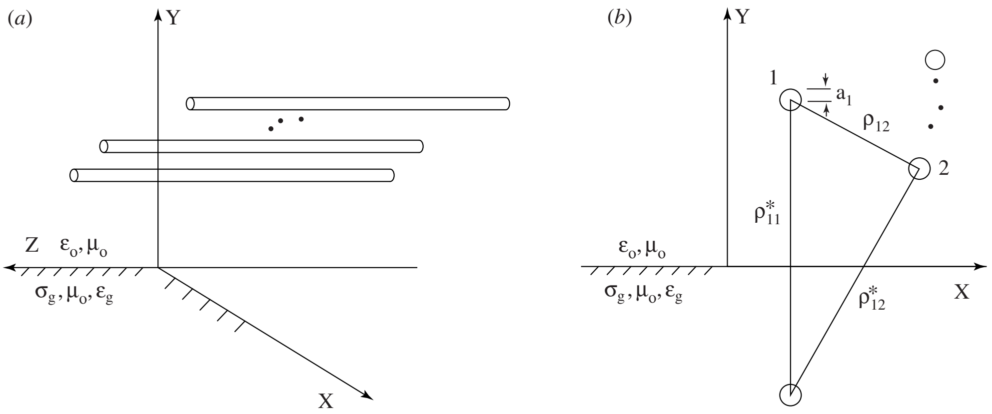

Figure 1. Transmission line geometry.

2. Transmission line parameters

The configuration of the transmission line is depicted in figure 1. A system of parallel thin wires is located in the air ($y > 0$), above a conducting earth ($y < 0$) with electrical parameters ε_g, μ_o and σ_g. The nth wire has a radius a_n, and is located at a height $y = y_n$, and a position $x = x_n$. The half-space ($y > 0$) is characterized by ε_o and μ_o. Note that for typical overhead communication cables and power lines, conductors are 5 m or more above ground while their radii may range from a few millimetres to a few centimetres.

According to Bridges *et al* [2], for such a structure, the unknown propagation constant k_z is a solution of the modal equation

$$\det([\boldsymbol{Z}_{\mathrm{ser}}] - [(\mathrm{i}k_z)^2]\,[\boldsymbol{Y}_{\mathrm{sh}}]^{-1}) = 0 \tag{1}$$

where

$$[\boldsymbol{Y}_{\mathrm{sh}}]^{-1}_{mn} = -\frac{1}{2\mathrm{i}\pi\omega\varepsilon_0}\frac{1}{\tau a_n \boldsymbol{K}_1(\tau a_n)} \times \left[\boldsymbol{K}_0(\tau\rho_{mn}) - \boldsymbol{K}_0(\tau\rho^*_{mn}) + \boldsymbol{G}(\tau, \rho^*_{mn})\right] \tag{2}$$

$$[\boldsymbol{Z}_{\mathrm{ser}}]_{mn} = [\boldsymbol{Z}_w]_{mn} - \frac{\mathrm{i}\omega\mu_0}{2\pi}\frac{1}{\tau a_n \boldsymbol{K}_1(\tau a_n)} \times \left[\boldsymbol{K}_0(\tau\rho_{mn}) - \boldsymbol{K}_0(\tau\rho^*_{mn}) + \boldsymbol{J}(\tau, \rho^*_{mn})\right] \tag{3}$$

$$\boldsymbol{J}(\tau, \rho^*_{mn}) = \int_{-\infty}^{+\infty} \frac{\exp(-u_o(y_n + y_m) - \mathrm{i}\lambda\,|x_n - x_m|)}{u_o + u_g}\,\mathrm{d}\lambda \tag{4}$$

$$\boldsymbol{G}(\tau, \rho^*_{mn}) = \int_{-\infty}^{+\infty} \frac{\exp(-u_o(y_n + y_m) - \mathrm{i}\lambda\,|x_n - x_m|)}{\boldsymbol{n}^2 u_o + u_g}\,\mathrm{d}\lambda \tag{5}$$

$$u_o = \sqrt{\tau^2 + \lambda^2} \qquad u_g = \sqrt{\tau_g^2 + \lambda^2}$$

$$\tau = \sqrt{k_z^2 - k_o^2} \qquad \tau_g = \sqrt{k_z^2 - k_g^2}$$

and

$$\rho_{mn} = \sqrt{(x_n - x_m)^2 + (y_n - y_m)^2}$$
$$\rho^*_{mn} = \sqrt{(x_n - x_m)^2 + (y_n + y_m)^2}.$$

The integration contour in (4) and (5) is the real axis of λ running from $-\infty$ to $+\infty$. In addition, to be definite, we choose the square root such that Re $(u_o) \geqslant 0$ for all real values of λ. When we deal with the region $y < 0$, the factor $\exp(+u_g y)$ appears in the solution. Again, for the sake of consistency we choose Re $(u_g) \geqslant 0$. The real parts of the transverse propagation constants τ and τ_g, in the air and in the ground, respectively, have been chosen to retain a positive value on the correct Riemann sheet Re $(\tau, \tau_g) \geqslant 0$.

The ground is assumed to be homogeneous and a complex refractive index $\boldsymbol{n}$ is defined for it as

$$\boldsymbol{n} = \sqrt{\varepsilon_g/\varepsilon_o + \mathrm{i}\frac{\sigma_g}{\omega\varepsilon_o}}$$

with Im $(\boldsymbol{n}) \geqslant 0$, appropriate to an $\exp(-\mathrm{i}\omega t)$ time dependence. $k_o = \omega\sqrt{\mu_o\varepsilon_o}$ is the propagation constant in air and $k_g = \sqrt{\omega^2\mu_o\varepsilon_g + \mathrm{i}\omega\mu_o\sigma_g}$ is the propagation constant in the ground. ω is the angular frequency.

$[\boldsymbol{Z}_w]$ is expressed in terms of modified Bessel functions and represents the internal impedance matrix [2]. $[\boldsymbol{Z}_{\mathrm{ser}}]_{mn}$ are the series impedance matrix elements, and $[\boldsymbol{Y}_{\mathrm{sh}}]_{mn}$ are the shunt admittance matrix elements of the transmission line. $\boldsymbol{G}$ and $\boldsymbol{J}$ are the Sommerfeld-type Fourier integrals [2, 4]. $\boldsymbol{K}_0(z)$ and $\boldsymbol{K}_1(z)$ are modified Bessel functions of the second kind.

3. Approximations of integrals

In the framework of the quasi-TEM approximation, the propagation constant k_z deviates little from the free-space value ($\tau \simeq 0$) [3]. Then the integrals (4) and (5) become

$$\boldsymbol{J}(X, Y) = \int_{-\infty}^{+\infty} \frac{\exp(-|\lambda|\,Y - \mathrm{i}\lambda X)}{|\lambda| + \sqrt{\lambda^2 - k_o^2(\boldsymbol{n}^2 - 1)}}\,\mathrm{d}\lambda \tag{6}$$

$$\boldsymbol{G}(X, Y) = \int_{-\infty}^{+\infty} \frac{\exp(-|\lambda|\,Y - \mathrm{i}\lambda X)}{\boldsymbol{n}^2\,|\lambda| + \sqrt{\lambda^2 - k_o^2(\boldsymbol{n}^2 - 1)}}\,\mathrm{d}\lambda \tag{7}$$

with $Y > 0$ and $X > 0$.

To find approximate analytic expressions of (6) and (7), we use the following approximation:

$$\begin{aligned} &\frac{u_o - u_g}{u_o + u_g} \simeq -\exp(-u_o Y_J) \\ &Y_J = \frac{2}{k_o\sqrt{1 - \boldsymbol{n}^2}} \end{aligned} \tag{8}$$

which is valid in the neighbourhood of $\lambda = 0$ as shown in the appendix. For small values of τ, the integrands in (6) and (7) decrease as $\exp(-|\lambda|\,Y)$ away from the point $\lambda = 0$. The major contribution to the integrals is then from the vicinity of $\lambda = 0$. Accurate analytical approximations of the previous integrals can, therefore, be obtained using (8). Note that the transverse propagation constant τ in the medium ($y > 0$) does not necessarily approach zero if the conditions of the quasi-TEM approximation are not satisfied. In this case the relationship is worst, and one cannot insert it directly in integrals (4) and (5) for arbitrary values of τ.

Based upon (8) and the following relationship:

$$\frac{1}{2u_o}\frac{u_o - u_g}{u_o + u_g} + \frac{1}{2u_o} = \frac{1}{u_o + u_g} \tag{9}$$

we may rewrite (6) as

$$\boldsymbol{J}(X, Y) \simeq \lim_{\tau \to 0}\left(\int_{-\infty}^{+\infty} \frac{\exp(-u_o Y - \mathrm{i}\lambda X)\,\mathrm{d}\lambda}{2u_o} - \int_{-\infty}^{+\infty} \frac{\exp(-u_o(Y + Y_J) - \mathrm{i}\lambda X)\,\mathrm{d}\lambda}{2u_o}\right). \tag{10}$$

The evaluation of the previous limit is accomplished by noting that

$$\int_{-\infty}^{+\infty} \frac{\exp(-u_o Y - \mathrm{i}\lambda X)}{2u_o}\,\mathrm{d}\lambda = K_o\left(\tau\sqrt{X^2+Y^2}\right) \tag{11}$$

and $K_o(z) \sim -\ln(z)$ for $z \to 0$ [5]. Combining the results (10) and (11), we obtain the following analytical approximation of (6) which is very convenient for evaluation:

$$\boldsymbol{J}(X,Y) \simeq \ln\left(\frac{\rho_J^*}{\rho^*}\right) \tag{12}$$

where

$$\rho_J^* = \sqrt{X^2 + (Y+Y_J)^2}$$
$$\rho^* = \sqrt{X^2+Y^2}.$$

We now deal with the integral (7). It is of interest to note that the same procedure leading to (12) can also be used to approximate (7).

After some algebraic manipulations, the remaining integral (7) is easily shown to be

$$\begin{aligned}\boldsymbol{G}(X,Y) &= \frac{2\boldsymbol{n}^2}{\boldsymbol{n}^4-1}\int_0^{+\infty}\frac{\exp(-k_oY\alpha)\cos(k_oX\alpha)}{\alpha-b}\,\mathrm{d}\alpha\\ &\quad -\frac{2}{\boldsymbol{n}^4-1}\int_0^{+\infty}\frac{\exp(-k_oY\alpha)\cos(k_oX\alpha)}{\alpha^2-b^2}\left(\sqrt{\alpha^2+1-\boldsymbol{n}^2}+\boldsymbol{n}^2b\right)\mathrm{d}\alpha\\ &= \boldsymbol{G}_o(X,Y)+\boldsymbol{G}_1(X,Y)\end{aligned} \tag{13}$$

where

$$\boldsymbol{G}_o(X,Y) = \frac{2\boldsymbol{n}^2}{\boldsymbol{n}^4-1}\int_0^{+\infty}\frac{\exp(-k_oY\alpha)\cos(k_oX\alpha)}{\alpha-b}\,\mathrm{d}\alpha \tag{14}$$

$$\boldsymbol{G}_1(X,Y) = -\frac{2}{\boldsymbol{n}^4-1}\int_0^{+\infty}\frac{\exp(-k_oY\alpha)\cos(k_oX\alpha)}{\alpha^2-b^2}\left(\sqrt{\alpha^2+1-\boldsymbol{n}^2}+\boldsymbol{n}^2b\right)\mathrm{d}\alpha \tag{15}$$

and

$$b = \mathrm{i}/\sqrt{1+\boldsymbol{n}^2}.$$

The integration corresponding to (14) may be accomplished in closed form. By using the definition for the exponential integral, we show in the appendix that (14) is simply given by

$$\boldsymbol{G}_o(X,Y) = \frac{\boldsymbol{n}^2}{\boldsymbol{n}^4-1}\left(\boldsymbol{Q}(bz)+\boldsymbol{Q}(b\bar{z})\right) \tag{16}$$

where $\boldsymbol{Q}(z) = \exp(-z)\boldsymbol{E}_1(-z)$. The exponential integral is defined by $\boldsymbol{E}_1(z) = \int_z^\infty \exp(-t)/t\,\mathrm{d}t$ [5, p 228]. $z = k_o(Y+\mathrm{i}X)$, and $\bar{z}$ is the complex conjugate of z.

Now, we consider the integral (15). By expressing the cosine function in terms of exponential functions we have

$$\boldsymbol{G}_1(X,Y) = -\frac{1}{\boldsymbol{n}^4-1}\left(\boldsymbol{G}_2(z)+\boldsymbol{G}_2(\bar{z})\right) \tag{17}$$

where

$$\boldsymbol{G}_2(z) = \boldsymbol{n}^2\int_0^\infty \frac{b\exp(-\alpha z)}{\alpha^2-b^2}\,\mathrm{d}\alpha + \int_0^\infty \frac{\sqrt{\alpha^2+1-\boldsymbol{n}^2}\exp(-\alpha z)}{\alpha^2-b^2}\,\mathrm{d}\alpha. \tag{18}$$

The first integral in (18) is elementary and can be expressed as

$$\boldsymbol{n}^2\int_0^\infty \frac{b\exp(-\alpha z)}{\alpha^2-b^2}\,\mathrm{d}\alpha = \frac{\boldsymbol{n}^2}{2}\left(\boldsymbol{Q}(bz)-\boldsymbol{Q}(-bz)\right) \tag{19}$$

while the determination of the second rests upon the evaluation of the integral

$$\boldsymbol{P}(b,z)=\int_0^\infty \frac{\sqrt{\alpha^2+1-\boldsymbol{n}^2}}{\alpha-b}\exp(-\alpha z)\,\mathrm{d}\alpha. \tag{20}$$

It is pointed out that the results in (16) and (19) are valid for Re $(z)>0$. This condition, which is necessary to ensure convergence of the integrals, is satisfied because Re $(z)=k_oY>0$.

Substitution of $\alpha=t\sqrt{1-\boldsymbol{n}^2}$ into the integral (20) yields

$$\boldsymbol{P}(b,z)=\sqrt{1-\boldsymbol{n}^2}\int_0^\infty \mathrm{e}^{\mathrm{i}\theta}\frac{\sqrt{1+t^2}}{t-b/\sqrt{1-\boldsymbol{n}^2}}\exp\left(-tz\sqrt{1-\boldsymbol{n}^2}\right)\mathrm{d}t \tag{21}$$

where $\theta=-\arg\sqrt{1-\boldsymbol{n}^2}$. Since Re $(\sqrt{1-\boldsymbol{n}^2})>0$ and Im $(\sqrt{1-\boldsymbol{n}^2})<0$ for all electrical parameters of the structure under consideration, we have $0<\theta<\pi/2$. The integration path $\arg t=\theta$ in (21) may be rotated back to the positive real axis if $-\pi/2+\theta<\arg z<\pi/2$. The resulting integral

$$\boldsymbol{P}(b,z)=\sqrt{1-\boldsymbol{n}^2}\int_0^\infty \frac{\sqrt{1+t^2}}{t-b/\sqrt{1-\boldsymbol{n}^2}}\exp\left(-tz\sqrt{1-\boldsymbol{n}^2}\right)\mathrm{d}t \tag{22}$$

is convergent for Re $(z\sqrt{1-\boldsymbol{n}^2})>0$, that is, for $-\pi/2+\theta<\arg z<\pi/2+\theta$. Then, by analytic continuation, the integral representation (22) for $\boldsymbol{P}(b,z)$ is valid for Re $(z\sqrt{1-\boldsymbol{n}^2})>0$.

Since the contribution to the integral (22) comes mainly from small t, it is more convenient to approximate $\sqrt{1+t^2}$ around $t=0$. An expression for this is found in the appendix. The result is repeated here as

$$\sqrt{1+t^2}\simeq\frac{1}{2t}+t-\frac{\exp(-2t)}{2t}. \tag{23}$$

Next, insert the approximation (23) for $\sqrt{1+t^2}$ into (22) and rewrite the integral as

$$\begin{aligned}\boldsymbol{P}(b,z)\simeq&-\frac{1-\boldsymbol{n}^2}{2b}\int_0^\infty\frac{1-\mathrm{e}^{-2t}}{t}\exp\left(-tz\sqrt{1-\boldsymbol{n}^2}\right)\mathrm{d}t\\&+\frac{1-\boldsymbol{n}^2}{2b}\int_0^\infty\frac{1-\mathrm{e}^{-2t}}{t-b/\sqrt{1-\boldsymbol{n}^2}}\exp\left(-tz\sqrt{1-\boldsymbol{n}^2}\right)\mathrm{d}t\\&+\sqrt{1-\boldsymbol{n}^2}\int_0^\infty\exp\left(-tz\sqrt{1-\boldsymbol{n}^2}\right)\mathrm{d}t+b\int_0^\infty\frac{\exp\left(-tz\sqrt{1-\boldsymbol{n}^2}\right)}{t-b/\sqrt{1-\boldsymbol{n}^2}}\mathrm{d}t.\end{aligned} \tag{24}$$

By a standard evaluation of the four integrals it is found that

$$\begin{aligned}\boldsymbol{P}(b,z)\simeq&-\frac{1-\boldsymbol{n}^2}{2b}\left(\ln\left(1+\frac{2}{z\sqrt{1-\boldsymbol{n}^2}}\right)+\boldsymbol{Q}\left(bz+\frac{2b}{\sqrt{1-\boldsymbol{n}^2}}\right)\right)\\&+\frac{1}{z}+b\boldsymbol{Q}(bz)\left(1+\frac{1-\boldsymbol{n}^2}{2b^2}\right).\end{aligned} \tag{25}$$

Finally, by combining (16)–(20), after some analytical manipulations we obtain

$$\begin{aligned}\boldsymbol{G}(X,Y)\simeq&\frac{\boldsymbol{n}^2}{2(\boldsymbol{n}^4-1)}(\boldsymbol{Q}(bz)+\boldsymbol{Q}(b\bar{z}))-\frac{1}{2b(\boldsymbol{n}^4-1)}(\boldsymbol{P}(b,z)+\boldsymbol{P}(b,\bar{z})-\boldsymbol{P}(-b,z)\\&-\boldsymbol{P}(-b,\bar{z})-\boldsymbol{n}^2b(\boldsymbol{Q}(-bz)+\boldsymbol{Q}(-b\bar{z})))\end{aligned} \tag{26}$$

where $P(b,z)$ is given by (25). It should be noticed that the approximation (25) is valid for Re $(z\sqrt{1-\boldsymbol{n}^2})>0$. In addition, when using the approximation for $\boldsymbol{P}$ in (26), it is required that Re $(z\sqrt{1-\boldsymbol{n}^2})>0$ and Re $(\bar{z}\sqrt{1-\boldsymbol{n}^2})>0$. This is equivalent to the conditions

$Y\mathrm{Re}\,(\sqrt{1-\boldsymbol{n}^2}) \mp X\mathrm{Im}\,(\sqrt{1-\boldsymbol{n}^2}) > 0$. The first condition, corresponding to the upper sign, is always satisfied because $X > 0$, $Y > 0$, $\mathrm{Re}\,(\sqrt{1-\boldsymbol{n}^2}) > 0$ and $\mathrm{Im}\,(\sqrt{1-\boldsymbol{n}^2}) < 0$. For most practical problems involving power lines and aerial communication cables, one may readily verify, within the framework of the quasi-TEM approximation, that the second condition is also satisfied. Indeed, in the case when the structure involves overhead lines, we have $Y > X$. Moreover, the use of the quasi-TEM approximation leads to $|\boldsymbol{n}| \gg 1$; this implies that $\mathrm{Re}\,(\sqrt{1-\boldsymbol{n}^2}) \simeq -\mathrm{Im}\,(\sqrt{1-\boldsymbol{n}^2})$. These two united conditions justify the validity of (26) for $Y > X$.

It can be seen that the result in (26) is expressed only in terms of logarithms and exponential integrals. The evaluation of (26) and (12) is, therefore, fast and may be achieved without numerical integration, if one uses a standard routine for evaluating $E_1(z)$ available in, for example, Mathematica. The numerical confirmation of the accuracy of these approximations by direct comparison with numerical values will be discussed in the next section.

4. Numerical results

In this section, we compare the values based on the analytical approximations with those obtained from numerical integration. We point out that the latter is accomplished by dividing the semi-infinite interval running from 0 to ∞ on the real axis into a number of equal subintervals and applying a Romberg integration algorithm to each. The numerical integration process stops when the contribution of the subinterval is too insignificant to be worth a special computation. The integrals are truncated at an upper limit λ_N. To speed up the convergence of the summation over the subintervals, Richardson extrapolation with respect to λ_N has been used.

As one can see, the previous integrals depend on X, Y, ω, ε_g and σ_g. X represents the horizontal distance between conductors, while Y designates the height above the ground. For practical interference problems involving above-ground cables, the largest value of Y is about 40 m. The smallest is 0.1 m or more. The ground conductivity σ_g varies from 0.1 m℧ m^{-1} to 0.1 ℧ m^{-1}. The range of values of the relative dielectric constant $\varepsilon_{rg} = \varepsilon_g/\varepsilon_o$ is from 5 to about 30. Generally, we have $X < Y$. Note that, when the ground is perfectly conducting ($\sigma_g \to \infty$), the integrals (6) and (7) vanish.

Now, consider figures 2 and 3, which show the integrals $\boldsymbol{J}$ and $\boldsymbol{G}$ computed from (12) and (26) versus those obtained from the numerical integration of (6) and (7). The configuration used for these cases (figures 2 and 3) is formed by a single conductor located at a height of 10 m above the ground. The electrical parameters of the ground are $\sigma_g = 0.01$ ℧ m^{-1}, $\varepsilon_{rg} = 15$ for figure 2 and $\sigma_g = 0.01$ ℧ m^{-1}, $\varepsilon_{rg} = 8$ for figure 3. This configuration corresponds to a typical power line. In figure 2, the real part and the imaginary part of the integral $\boldsymbol{G}$ have been drawn as functions of the frequency $f = \omega/2\pi$. The dashed curve indicates the real part of $\boldsymbol{G}$, while the imaginary part is represented by the solid curve. Numerical and analytical curves are superimposed. Figure 3 shows that the numerical and analytical values of $\boldsymbol{J}$ are in good agreement.

To establish the accuracy of (12) and (26), calculations were performed using different parameters and the results are shown in table 1. It is seen from this table that the analytical values are accurate. Moreover, the computation times of the analytical approximations are quasi-independent of the parameters and are much smaller than the times consumed in numerical integration. It is important to note that this difference arises because the effective length of the integration interval λ_N changes as a function of the parameters. For example, λ_N increases as the frequency f decreases. As a result, the number of interval subdivisions increases.

For the parameters summarized in table 1, one can see that for calculating $\boldsymbol{J}$ using the

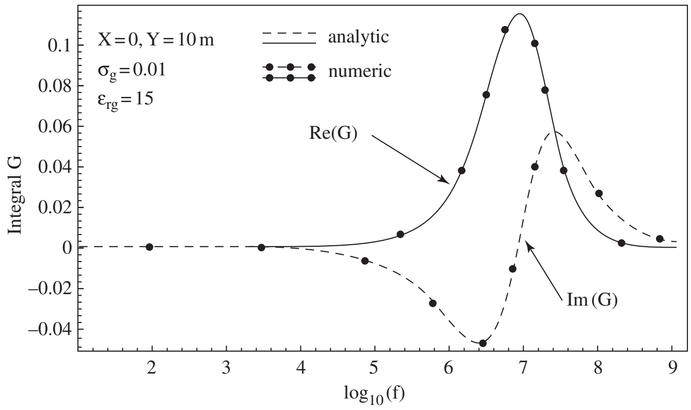

Figure 2. Comparison of analytical values of ***G*** with those obtained by numerical integration.

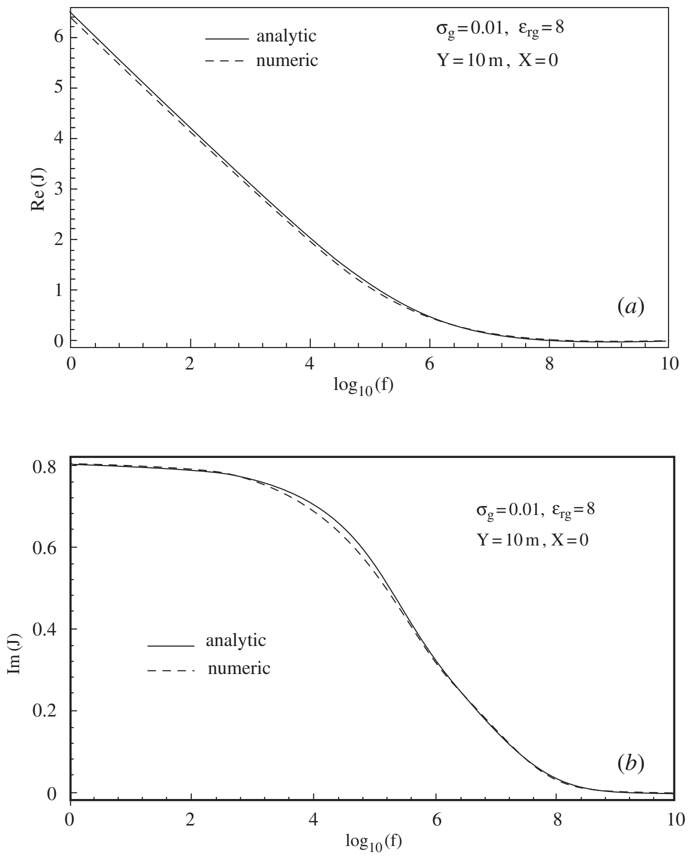

Figure 3. (*a*) Comparison of analytical and numerical values of Re (***J***). (*b*) Comparison of analytical and numerical values of Im (***J***).

numerical integration, the computation times are increased by a factor of 4.5–13.6, while ***G*** is computed up to 38 times faster with our method.

Table 1. Comparison of analytical and numerical values of integrals $\boldsymbol{J}$ and $\boldsymbol{G}$. CPU times are for a 486/100 MHz processor.

f (Hz)	X (m)	Y (m)	ε_{rg}	σ_g	$\boldsymbol{J}$ (anal)	$\boldsymbol{J}$ (num)	$\boldsymbol{G}$ (anal)	$\boldsymbol{G}$ (num)
10^3	0	10	15	10^{-2}	3.145	3.077	2.529E−5	2.529E−5
					+0.754i	+0.747i	−1.5E−4i	−1.5E−4i
	CPU (s)	→			0.15	1.68	0.37	14.30
10^4	5	10	10	10^{-2}	1.950	1.900	2.534E−4	2.534E−4
					+0.693i	+0.676i	−1.117E−3i	−1.117E−3i
	CPU (s)	→			0.15	1.57	0.37	12.22
10^4	7	10	10	10^{-3}	2.945	2.878	2.578E−3	2.578E−3
					+0.758i	+0.748i	−9.831E−3i	−9.831E−3i
	CPU (s)	→			0.15	1.74	0.37	8.06
10^6	8	20	5	10^{-2}	0.212	0.212	2.447E−2	2.447E−2
					+0.183i	+0.182i	−2.955E−2i	−2.956E−2i
	CPU (s)	→			0.15	0.66	0.37	8.06
10^4	0	0.2	10	10^{-3}	7.026	6.950	2.605E−3	2.6049E−3
					+0.7871i	+0.7869i	−1.424E−2i	−1.424E−2i
	CPU (s)	→			0.14	1.9	0.36	14
10^6	0	0.1	10	10^{-2}	4.187	4.274	2.976E−2	2.975E−2
					+0.7961i	+0.799i	−8.66E−2i	−8.65E−2i
	CPU (s)	→			0.16	1.75	0.54	10.53

5. Conclusion

In this paper, simple and accurate analytical approximations for integrals arising from the transmission line theory, under the quasi-TEM hypothesis, were derived. These formulae are valid for all their arguments and provide very accurate results using only elementary functions, and thus are very convenient when quick calculations are needed.

Appendix

Consider the relationship (8). The term on the left can be expanded into a Taylor series in u_o as

$$\begin{aligned}
\frac{u_o - u_g}{u_o + u_g} &= \frac{u_o - \sqrt{u_o^2 + \tau_g^2 - \tau^2}}{u_o + \sqrt{u_o^2 + \tau_g^2 - \tau^2}} \\
&= \frac{u_o - \sqrt{u_o^2 + k_o^2 - k_g^2}}{u_o + \sqrt{u_o^2 + k_o^2 - k_g^2}} \\
&= \frac{u_o - \sqrt{u_o^2 + k_o^2(1 - \boldsymbol{n}^2)}}{u_o + \sqrt{u_o^2 + k_o^2(1 - \boldsymbol{n}^2)}} \\
&= \frac{u_o - \sqrt{u_o^2 + 4/Y_J^2}}{u_o + \sqrt{u_o^2 + 4/Y_J^2}} \\
&= -1 + Y_J u_o - \tfrac{1}{2} Y_J^2 u_o^2 + \tfrac{1}{8} Y_J^3 u_o^3 + \mathrm{O}(u_o^4)
\end{aligned}$$

since the contribution to integrals (4) and (5) is from the vicinity of $\lambda = 0$.

Neglecting the cubic term, we can easily show that

$$-\exp(-Y_J u_o) \simeq -1 + Y_J u_o - \frac{1}{2}Y_J^2 u_o^2 \simeq \frac{u_o - u_g}{u_o + u_g}.$$

Similarly, it is clear that in the vicinity of $t = 0$, we have

$$\frac{t - \sqrt{1+t^2}}{t + \sqrt{1+t^2}} \simeq -\exp(-2t)$$

which is equivalent to

$$2t^2 + 1 - 2t\sqrt{1+t^2} \simeq \exp(-2t).$$

By extracting the square-root term, we find that

$$\sqrt{1+t^2} \simeq t + \frac{1}{2t} - \frac{\exp(-2t)}{2t}.$$

Now, consider the integral (14). By expressing the cosine function in terms of exponential functions, we get

$$\frac{\boldsymbol{n}^2}{\boldsymbol{n}^4 - 1}\int_0^\infty \left(\frac{\exp(-k_o(Y + \mathrm{i}X)\alpha)}{\alpha - b} + \frac{\exp(-k_o(Y - \mathrm{i}X)\alpha)}{\alpha - b}\right) \mathrm{d}\alpha$$
$$= \frac{\boldsymbol{n}^2}{\boldsymbol{n}^4 - 1}\int_0^\infty \left(\frac{\exp(-z\alpha)}{\alpha - b} + \frac{\exp(-\overline{z}\alpha)}{\alpha - b}\right) \mathrm{d}\alpha$$

with $\mathrm{Re}\,(z) > 0$. For the first term in the integrand, let $t = (\alpha - b)z$ and for the second term, let $t = (\alpha - b)\overline{z}$, then

$$\boldsymbol{G}_o = \frac{\boldsymbol{n}^2}{\boldsymbol{n}^4 - 1}\left(\exp(-bz)\int_{-bz}^\infty \frac{\exp(-t)}{t}\,\mathrm{d}t + \exp(-b\overline{z})\int_{-b\overline{z}}^\infty \frac{\exp(-t)}{t}\,\mathrm{d}t\right).$$

Hence, from [5],

$$\boldsymbol{G}_o = \frac{\boldsymbol{n}^2}{\boldsymbol{n}^4 - 1}\left(\exp(-bz)E_1(-bz) + \exp(-b\overline{z})E_1(-b\overline{z})\right) = \frac{\boldsymbol{n}^2}{\boldsymbol{n}^4 - 1}\left(\boldsymbol{Q}(bz) + \boldsymbol{Q}(b\overline{z})\right).$$

References

[1] Carson J R 1926 Wave propagation in overhead wires with ground return *Bell Syst. Tech. J.* **5** 539–54

[2] Bridges G E, Aboul-Atta O and Shafai L 1988 Solution of discrete modes for wave propagation along multiple conductor structures above a dissipative Earth *Can. J. Phys.* **66** 428–38

[3] Zeddam A, Koné I, Deguauque P and Demoulin B 1988 Voltages induced on coaxial cables or multi-wire shielded lines by a disturbing wave *Electromagnetics* **8** 311–33

[4] Amri A and Maaouni A 1996 Evaluation numérique des intégrales de Sommerfeld du type Fourier dans le plan complexe *Ann. Telecommun.* **51** 4–10

[5] Abramowitz M and Stegun I 1964 *Handbook of Mathematical Functions* (Washington, DC: National Bureau of Standards)